Computer-generated holograms of images reconstructed on curved surfaces

Joseph Rosen

When one illuminates a computer-generated hologram by a plane wave, the obtained two-dimensional image is usually displayed on a planar plane. Other possibilities for reconstructing images on arbitrary curved surfaces are discussed herein. As an example, the reconstruction of an image on a virtual spherical surface is demonstrated. © 1999 Optical Society of America

OCIS codes: 090.1760, 070.2580, 070.2590, 050.1970, 090.2870.

1. Introduction

A computer-generated hologram (CGH) is most commonly a transmission mask employed to reconstruct a desired image on a transverse planar plane located some distance from the hologram plane. The problem of reconstructing two-dimensional (2-D) images from CGH's on arbitrary virtual curved surfaces is considered in this paper. Reconstruction of a 2-D image on a curved surface actually creates a three-dimensional (3-D) display. Therefore this technique may play an important role in attempts at efficient reconstruction of 3-D images from CGH's.[1] Synthesizing CGH's for general arbitrary 3-D images is usually a heavy computational task, and for many years researchers have searched for various methods to ease this computational problem.[1] In the early days of CGH's Waters calculated a CGH as the sum of aperture functions corresponding to each of the points of a 3-D object.[2] In another pioneering study Leseberg and Frère demonstrated an image reconstruction from a Fresnel CGH on a tilted planar plane, using fast Fourier transform (FFT).[3] In two other papers[4,5] the authors proposed to superpose a few CGH's, each for a different shifted and tilted reconstruction plane, and consequently a complicated 3-D image could be obtained. A natural extension of these studies leads us to propose, in the following, displaying the reconstructed image on an arbitrary curved surface. In addition to the obvious use of these CGH's to create 3-D holographic displays, this technique may be applied for interferometric tests.[6] Such a CGH can simulate arbitrary curved surfaces for comparison with manufactured surfaces for industrial quality control.

2. General Analysis

The holograms in the present study are Fourier holograms, displayed on the front focal plane of a spherical lens, and the reconstructed images are obtained at the vicinity of the rear focal plane. The setup of the CGH is shown in Fig. 1. The CGH is displayed on plane P_1 with the coordinates (u, v) and illuminated by a plane wave. The reconstructed image is displayed on a curved surface P_c at the vicinity of the rear focus of the lens. This focal point is used as the origin of the coordinate system (x, y, z). Let us first look at a single image point (x, y, z) from the entire reconstructed image. In the frame of the Fresnel approximation each image point is obtained by illumination of a plane wave on the phase transparency

$$A \exp\left[j\, \frac{\pi z(u^2 + v^2)}{\lambda f^2} - j\, \frac{2\pi}{\lambda f}(xu + yv)\right]$$

in the (u, v) plane.[7] A is some complex constant, λ is the wavelength, and f is the focal distance of the lens. The use of the Fresnel approximation is justified under the assumptions that the focal distance is much longer than the aperture size and that any image point is not far from the optical axis. Assuming that all of the image points on the curved surface are arranged on a matrix of size $N \times M$, the desired overall distribution of the hologram $h(u, v)$ is ob-

The author is with the Department of Electrical and Computer Engineering, Ben-Gurion University of the Negev, P.O. Box 653, Beer-Sheva 84105, Israel. His e-mail address is rosen@ee.bgu.ac.il.
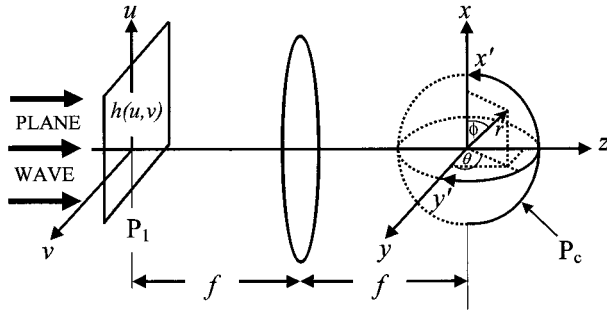
Fig. 1. Optical setup used to obtain an image reconstruction from the CGH on a virtual spherical surface.

tained by summation over $N \times M$ phase functions as follows:

$$h(u, v) = \sum_n^N \sum_m^M A_{nm} \exp\left[j \frac{\pi z_{nm}(u^2 + v^2)}{\lambda f^2} - j \frac{2\pi}{\lambda f}(x_{nm}u + y_{nm}v)\right].$$ (1)

When the distances between all the points located on the curved surface approach zero, the sum can be replaced by the following integral:

$$h(u, v) = \int\int A(x', y') \exp\left\{j \frac{\pi z(x', y')(u^2 + v^2)}{\lambda f^2} - j \frac{2\pi}{\lambda f}[x(x', y')u + y(x', y')v]\right\} \mathrm{d}x'\mathrm{d}y',$$ (2)

where (x', y') are the transverse coordinates of the curved surface. Equation (2) is actually the general guideline for computing the CGH $h(u, v)$ to construct the image $A(x', y')$ on the virtual curved surface P_c, defined by the functions $x(x', y')$, $y(x', y')$, and $z(x', y')$.

Equation (2) can be calculated efficiently with the FFT algorithm if it can be rewritten in the form of a 2-D Fourier transform. This can happen if and only if the function $z(x', y')$ is a linear combination of the form

$$z(x', y') = ax(x', y') + by(x', y') + c,$$
$$\forall (x', y') \in P_c,$$ (3)

where a, b, c are some real constants. This condition is satisfied if and only if $x(x', y')$, $y(x', y')$, and $z(x', y')$ are linear functions of (x', y') or, in another words, only when the reconstruction surface is a tilted planar plane.[3–5]

If the reconstruction plane is some arbitrary nonplanar surface, Eq. (2) cannot be presented as a 2-D Fourier transform and thus we cannot use the FFT algorithm. Until a better way is suggested, the CGH of an image, reconstructed on an arbitrary curved surface, can be computed directly only from its definition given by Eq. (2). Apparently the direct CGH calculation is a return to the early method of

Waters[2]; however, there are a few significant differences between his and the present methods. From Eq. (2) it is obvious that the integration here is over a surface instead of over the whole volume. The computational algorithm gets any 2-D image as an input and without any further preprocessing yields the desired CGH of that image displayed on the given curved surface. The computation time can be significantly reduced if the reconstruction surface is cylindrical, i.e., if the nonplanar curve exists only in one of the transverse dimensions. In this case one can calculate one integral of Eq. (2) by the one-dimensional FFT algorithm, whereas the other should still be calculated directly from the definition.

3. Spherical Display

As an example of a nonplanar reconstruction surface we chose the spherical surface shown in Fig. 1. The focal point is used as the sphere center, its radius is r, and the angles (ϕ, θ) are defined in the figure. Since the arc's length of a circle is equal to the product of the radius by the arc's angle, the coordinates of the spherical surface are given by

$$x' = r[(\pi/2) - \phi],$$
$$y' = r[(\pi/2) - \theta],$$ (4)

where we choose $-r\pi/2 \leq x' \leq r\pi/2$ and $-r\pi/2 \leq y' \leq r\pi/2$. Next we use the transformation relations between Cartesian coordinates (x, y, z) and spherical coordinates (r, ϕ, θ) and substitute Eqs. (4) into these relations. Therefore the rear focal space coordinates (x, y, z) as a function of the image coordinates (x', y') are given by

$$x = r\cos(\phi) = r\sin(x'/r),$$
$$y = r\cos(\theta)\sin(\phi) = r\sin(y'/r)\cos(x'/r),$$
$$z = r\sin(\theta)\sin(\phi) = r\cos(y'/r)\cos(x'/r).$$ (5)

Substituting Eqs. (5) into Eq. (2) yields

$$h(u, v) = \int\int A(x', y')\exp\left\{j\cos\left(\frac{y'}{r}\right)\right.$$
$$\times \cos\left(\frac{x'}{r}\right)\frac{\pi r(u^2 + v^2)}{\lambda f^2}$$
$$- j\frac{2\pi r}{\lambda f}\left[\sin\left(\frac{x'}{r}\right)u + \sin\left(\frac{y'}{r}\right)\right.$$
$$\left.\left.\times \cos\left(\frac{x'}{r}\right)v\right]\right\}\mathrm{d}x'\mathrm{d}y'.$$ (6)

$h(u, v)$ is the desired hologram distribution for reconstructing the 2-D image $A(x', y')$ on the virtual spherical surface P_c with the Cartesian coordinates (x', y').

4. Simulation Results

The binary image shown in Fig. 2 was used as the pattern to be displayed on the spherical surface. This image was multiplied by a random phase distribution to obtain a function $h(u, v)$ with a closely uniform magnitude. The function $A(x', y')$ com-

Fig. 2. Binary image used for the CGH design and aimed to be displayed on the spherical surface.

Fig. 3. Upper left-hand corner of the synthesized gray-scale CGH (128×128 pixels out of 512×512 pixels).

posed from the magnitude (shown in Fig. 2) and the random phase were substituted into Eq. (6) to calculate the complex transparency $h(u, v)$. $h(u, v)$ was calculated directly from Eq. (6) without use of the FFT algorithm.

When the holographic medium cannot function as a complex modulator, the complex function $h(u, v)$ should be coded as a real positive transparency. This coding process is performed such that the obtained hologram is

$$h_r(u, v) = 1 + \text{Re}\left\{ h(u, v)\exp\left[\frac{j2\pi}{\lambda f}(d_x u + d_y v)\right]\right\}, \quad (7)$$

where $(d_x, d_y, 0)$ is the new origin point of the reconstruction space. Part of the final hologram synthesized according to Eqs. (6) and (7) is shown in Fig. 3. The hologram was designed for a spherical surface of radius $r = 2$ cm with the parameters $\lambda = 0.63$ μm, $f = 4$ m, a transverse size of 1 cm $\times$ 1 cm, and 512×512 pixels on the hologram. Illuminating this hologram, located at plane P_1, by a plane wave yields the desired object displayed on the virtual spherical surface.

The simulation result of the optical diffraction on the plane $z = 20$ mm, by use of a Fresnel propagator, is shown in Fig. 4. Only the central part of the image in the first diffraction order is in focus at this distance behind the focal plane. In Fig. 5 we see the intensity distribution of the first diffraction order, on nine different transverse planes along the propagation axis z, behind the rear focus, between $z = 4$ mm and $z = 20$ mm. Note that, since the image is displayed on a spherical surface, in each figure a different annular section of the image is in focus.

Implementation of a binary hologram for the same purposes was also examined in this study. The binary hologram $h_b(u, v)$ can be easily obtained from
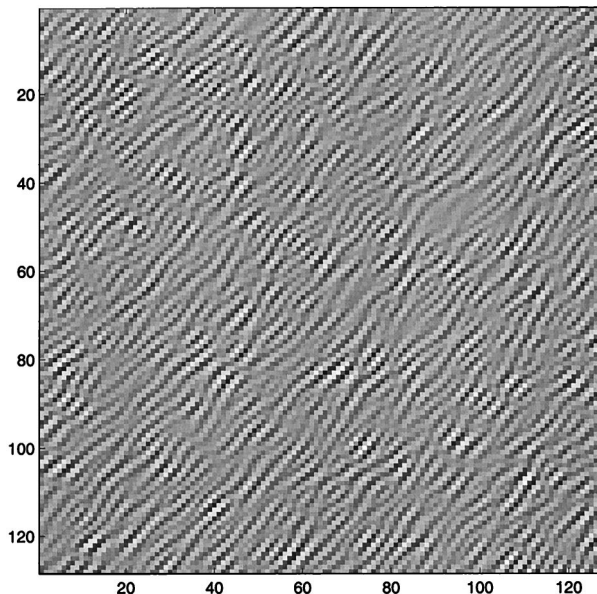
the original complex hologram $h(u, v)$ according to the rule

$$h_b(u, v) = \begin{cases} 1 & \text{Re}\left\{ h(u, v)\exp\left[\dfrac{j2\pi}{\lambda f}(d_x u + d_y v)\right]\right\} > 0 \\ 0 & \text{otherwise} \end{cases}.$$

$$(8)$$

Part of the final hologram synthesized according to Eqs. (6) and (8), with the same design parameters mentioned above, is shown in Fig. 6. The diffraction pattern on the plane $z = 20$ mm behind the rear focal
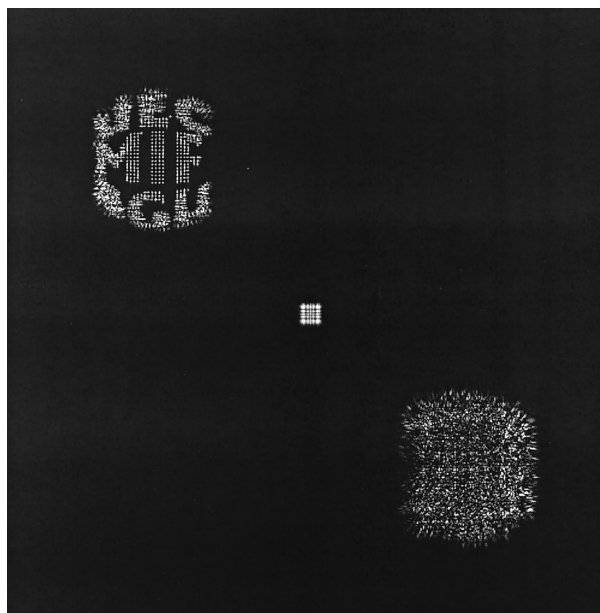

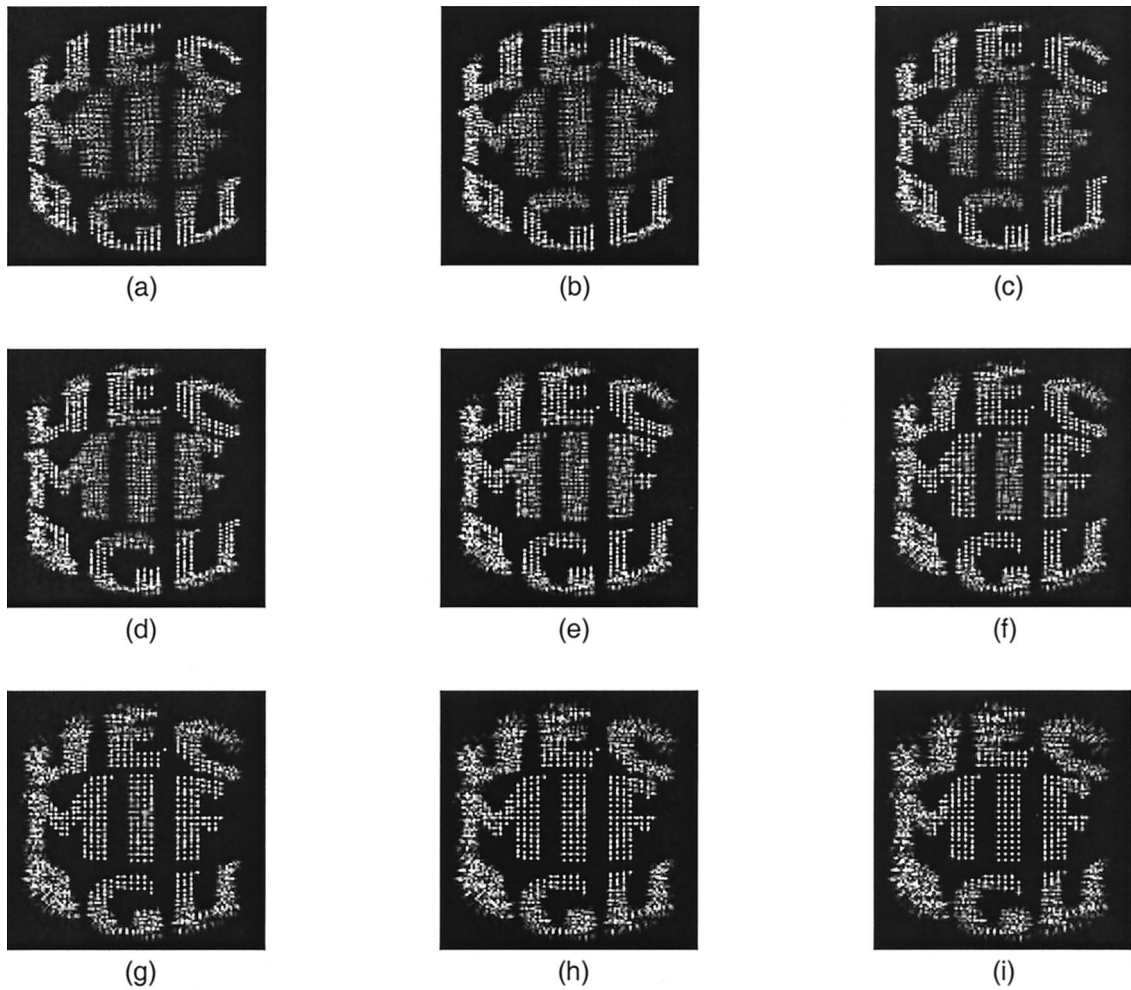Fig. 4. Reconstruction results from the gray-scale CGH on the plane $z = 20$ mm behind the rear focal plane.

Fig. 5. Reconstruction results from the gray-scale CGH, in the first diffraction order, behind the rear focus, on the transverse planes: (a) $z = 4$ mm, (b) $z = 6$ mm, (c) $z = 8$ mm, (d) $z = 10$ mm, (e) $z = 12$ mm, (f) $z = 14$ mm, (g) $z = 16$ mm, (h) $z = 18$ mm, (d) $z = 20$ mm.
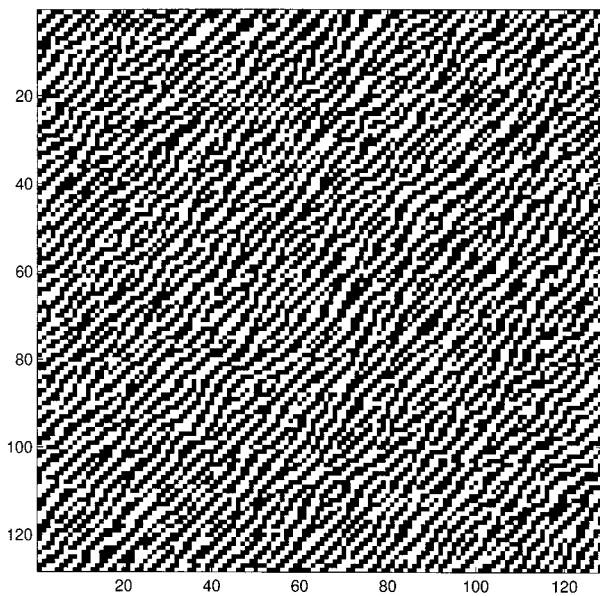

Fig. 6. Upper left-hand corner of the synthesized binary CGH (128×128 pixels out of 512×512 pixels).
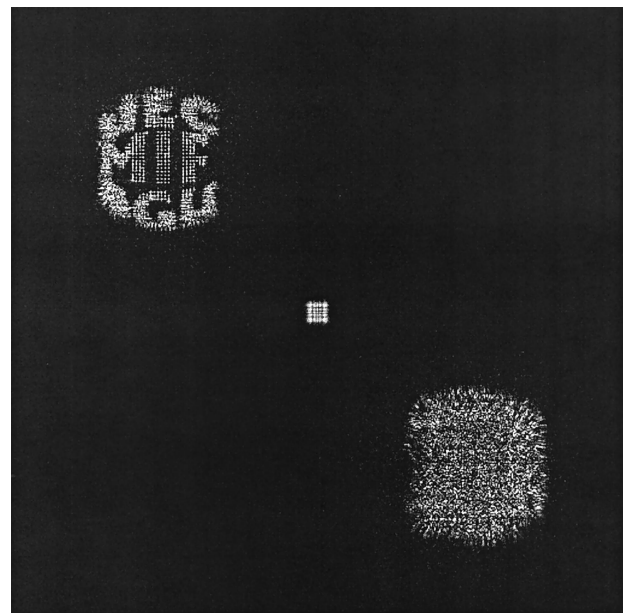

Fig. 7. Reconstruction results from the binary CGH on the plane $z = 20$ mm behind the rear focal plane.

plane, which resulted from binary hologram $h_b(u, v)$, is shown in Fig. 7. This result is slightly more clattered than the diffraction result from the gray-scale hologram. In the case in which the magnitude of the complex function $h(u, v)$ is closely uniform, the binary function $h_b(u, v)$ is a good approximation of the gray-scale function $h_r(u, v)$, and therefore the diffraction results are quite similar. In the other case, in which the object is not multiplied by a random phase, and as a result $h(u, v)$'s magnitude is far from being uniform, a more sophisticated binarization method should be applied to achieve similar results.

5. Conclusions

In conclusion, a method to design CGH's for displaying 2-D images on arbitrary curved surfaces has been introduced and demonstrated. The key point of this method is to identify the relations between the transverse coordinates of the curved surface and the Cartesian coordinates of the reconstruction scene. These relations are substituted into the formula (Eq. 2), which relates between the transparency on the front focal plane and the image on the curved surface around the rear focus.

References

1. O. Bryngdahl and F. Wyrowski, "Digital holography/computer-generated holograms," in *Progress In Optics*, E. Wolf, ed. (North-Holland, Amsterdam, 1990), Vol. 28, pp. 1–86.
2. J. P. Waters, "holographic image synthesis utilizing theoretical methods," Appl. Phys. Lett. **9,** 405–407 (1966).
3. D. Leseberg and C. Frère, "Computer-generated holograms of 3-D objects composed of tilted planar segments," Appl. Opt. **27,** 3020–3024 (1988).
4. C. Frère and D. Leseberg, "Large objects reconstructed from computer-generated holograms," Appl. Opt. **28,** 2422–2425 (1989).
5. T. Tommasi and B. Bianco, "Computer-generated holograms of tilted planes by a spatial-frequency approach," J. Opt. Soc. Am. A **10,** 299–305 (1993).
6. J. S. Loomis, "Computer-generated holography and optical testing," Opt. Eng. **19,** 679–685 (1980).
7. J. W. Goodman, *Introduction to Fourier Optics*, 2nd ed. (McGraw-Hill, New York, 1996), Chap. 5, p. 104.